

Supplementary Material: “Climate change decouples drought from early winegrape harvests in France”

Benjamin I Cook^{1,2} & Elizabeth M Wolkovich^{3,4}

December 3, 2015

Regional Harvest Date Analyses

To analyze each region individually, we regressed each harvest date time series used in GHD-Core against CRU climate data averaged within one degree of that site location. As with GHD-Core, temperature is the dominant control on harvest in all eight regional series (Supplementary Figures 4–11), and all the temperature regressions are highly significant ($p \leq 0.01$). For the period 1901–1980, the temperature sensitivities (regression slopes) across sites range from -3.70 days $^{\circ}\text{C}^{-1}$ at SRv to -7.39 days $^{\circ}\text{C}^{-1}$ at Cha1. Significant ($p \leq 0.05$) moisture sensitivities (precipitation and PDSI) are also found at seven of the eight sites: Als, Bor, Bur, Cha1, Lan, LLV, and Swi. At the eighth site, SRv, the precipitation regression is marginally significant ($p = 0.055$) and is insignificant for PDSI.

At all sites, temperature sensitivities are still significant for the 1981–2007 interval, indicating that temperature remains an important control on winegrape phenology in more recent decades. By contrast, most sites show a significant weakening of the two moisture sensitivities. Both the precipitation and PDSI regressions with harvest dates become (or remain) insignificant ($p > 0.05$) during 1981–2007 for Bor, Bur, Cha1, Lan, LLV, and Swi. At SRv, precipitation was already only marginally significant for 1901–1980, and this regression weakens considerably. At Als, the PDSI regression becomes insignificant, while precipitation does not change appreciably. Analyses of the individual regional harvest date series therefore support the general conclusions drawn from analyses of the

GHD-Core composite index, demonstrating an overall large-scale weakening of moisture controls on grape harvest dates in France and Switzerland.

Temperature versus Moisture Comparisons

We hypothesize that, in Western Europe, moisture impacts on winegrape phenology occur primarily through the indirect effect of moisture on growing season temperatures. Further, we argue that because of anthropogenic warming trends in recent decades, winegrape phenology has become decoupled from moisture variability. Here we, present evidence in support of these hypotheses.

A strong connection between soil moisture and warm season temperatures over the Mediterranean and Western Europe has been well established (1, 2), occurring primarily through the control of soil moisture on surface energy partitioning. In regions where evapotranspiration is limited by the supply of moisture at the surface, wetter soils will lead to increases in evapotranspiration and latent heat flux at the expense of sensible heating, keeping surface soil and air temperatures relatively cool. Conversely, if soils are dry, sensible heat fluxes will dominate, and soil and air temperatures will be higher. If these are the primary physics operating in our GHD-Core region, we would therefore expect negative relationships between temperature and precipitation or PDSI during the spring and summer.

Indeed, for both MJJ (Supplementary Figure 12) and JJA (Supplementary Figure 14) we can see significant negative relationships between both temperature and precipitation and PDSI during the 1901–1980 interval. The relationships are generally stronger during JJA, when solar energy inputs are larger and land-atmosphere interactions are expected to be stronger. During the more recent interval (1981–2007), the temperature-moisture relationships generally weaken, especially during JJA. Additionally, temperatures during 1981–2007 are substantially warmer compared to 1901–1980, reflecting recent warming trends driven primarily by anthropogenic greenhouse gas forcing. This additional warmth (unrelated to moisture variability), combined with the apparent weakening of the temperature-moisture coupling strength itself, supports our conclusions regarding the mechanisms by which moisture influences grape harvest date variability and the recent weakening of this relationship.

Resampling Analyses

Interpretations of the composite climate anomaly analyses (Figure 4, main manuscript) and comparisons of climate distributions (Supplemental Figure 15, top panel) for extreme early harvest years may be affected by sampling uncertainties or biases, especially during the post 1980 period when the number of years to sample from is small. For example, from 1600–1980, 72 years qualify as early harvests with GHD-Core anomalies of -7.67 days or earlier. Because of the terminal years in the climate reconstructions (2012 for PDSI, 2002 for temperature, 2000 for precipitation), however, from 1981 to 2007 only 18 years qualify for PDSI, 13 years for temperature, and 11 years for precipitation. To estimate the impact on our analyses of these potential sampling uncertainties, we conducted a resampling analysis where, in each of 10,000 iterations, we resampled climate anomalies from the early harvest years with replacement for the 1600–1980 period. In each iteration, we resampled n times, where n is equal to the number of early harvest years from 1981–2007 (so 11 for precipitation, 13 for temperature, and 18 for PDSI).

Kernal density functions for the 10,000 resampled mean precipitation and PDSI anomalies are shown in the bottom panels of Supplemental Figure 15. As in the main analysis, PDSI shows the strongest shift with early harvest dates before and after 1980. Repeating the One Sided Student's t-test during each of these iterations found significant differences ($p \leq 0.05$) in 99% of cases, indicating our earlier finding (drought, as represented by PDSI, is no longer associated with early harvests post-1980) is quite robust. The resampling results were not as robust for precipitation: only 29% of the iterations found marginally significantly ($p \leq 0.10$) drier conditions during the pre-1980 period compared to post-1980. In the precipitation reconstruction, however, we are severely limited in our sample size post-1980 (only 11 years, compared to 18 for PDSI). Our conclusions, however, are still strongly supported by both the observational analysis (using 20th century climate data) and the PDSI reconstruction.

Clonal Analyses

Selection of superior clonal material by managers may introduce changes over time that could influence vine phenology and harvest date. [LIZZIE INPUT HERE ON LANGUEDOC ETC]. To test for the potential impact of clonal selection on harvest dates, we refitted the Lan (Supplemental Figure 16) and GHD-Core (Supplemental Figure 17) regression models for three intervals across which

significant clonal selection is thought to have occurred: 1947–1957, 1958–1969, and 1970–1980. Compared to the regressions using more of the available data (e.g., Lan in Supplemental Figure 8 and GHD-Core in Figure 3 from the main manuscript) the results are noisier and less significant, as expected. For both sites, however, the temperature sensitivities for both Lan and GHD-Core are similar when comparing across these 11-year intervals and previous regressions (1901–1980 and 1981–2007). Combined with our focus on GHD-Core (which should minimize local management changes), we find it unlikely that clonal selection has had a significant impact on our results.

Phylloxera

In 1850s or 1860s, an exotic species of aphid (commonly known as grape phylloxera) was introduced to Europe. This resulted in a severe blight and destruction of many vineyards across France. Large-scale recovery of the vineyards and wine industry began in the late 1800s and early 1900s with the grafting of European vines onto phylloxera resistant root stock from the United States. There was thus a substantial shift in root stock composition beginning around the turn of the 20th century, a change that could conceivably affect our interpretation of climatic effects on harvest date.

To investigate this, we calculated regression models between GHD-Core and JJA climate (temperature, precipitation, PDSI) from the climate reconstructions (instrumental data is not available prior to 1901) (Supplemental Figure 18). Shown are three intervals: 1800–1850 (prior to the phylloxera epidemic), 1851–1900 (during the phylloxera epidemic), and 1901–1980 (after widespread grafting occurred). Results are generally consistent across all three time periods. For temperature, sensitivities, range from -4.97 to -6.56 days $^{\circ}\text{C}^{-1}$ with R^2 values from 0.359 to 0.464, similar to results found in the instrumental regressions for this season (Supplemental Figure 13). Similar results are found for precipitation and PDSI, although precipitation is only marginally significant for 1800–1850 (PDSI is still highly significant for this period, however). Given the lack of evidence for any systematic change in sensitivities pre- and post- phylloxera, we conclude that this event is unlikely to have significantly affected our climate based analyses and interpretations.

Multiple Regression Analyses

Temperature, precipitation, and PDSI are all significant predictors of grape harvest dates. However, it is unclear if moisture availability (as expressed by precipitation and PDSI) acts directly on grape phenology or indirectly through modulation of temperatures. To test this, we have conducted a multiple regression analysis to investigate if significant skill is added into the model when precipitation and PDSI are included as predictors with temperature.

Results from the single and multiple variable regressions (climate data from the instrumental CRU climate grids) are shown in Tables 9 (for 1901–1980) and 10 (1981–2007). Temperature is by far the single best predictor of harvest date; precipitation and PDSI are also significant predictors in their own single variable regressions. Adding precipitation and PDSI into the temperature regression model, however, does not substantially improve the explanatory power of the model (R^2) and these additional moisture terms are insignificant ($p > 0.05$). This suggest that moisture variability does not affect grape phenology directly but, instead, acts through the modulation of temperatures (where drier equals warmer, via the mechanisms discussed previously).

References

1. Fischer, E. M., Seneviratne, S. I., Vidale, P. L., Lüthi, D. & Schär, C. Soil Moisture–Atmosphere Interactions during the 2003 European Summer Heat Wave. *Journal of Climate* **20**, 5081–5099 (2007). URL <http://dx.doi.org/10.1175/JCLI4288.1>.
2. Miralles, D. G., Teuling, A. J., van Heerwaarden, C. C. & Vila-Guerau de Arellano, J. Mega-heatwave temperatures due to combined soil desiccation and atmospheric heat accumulation. *Nature Geoscience* **7**, 345–349 (2014). URL <http://dx.doi.org/10.1038/ngeo2141>.

Table 1: Regional grape harvest date series from DAUX used in construction of the GHD-Core composite series. Included are the three letter codes for each site, their geographic locations (units of decimal degrees), and their mean harvest dates (day of year) for various intervals.

GHD Series	Site Code	Lat	Lon	1600-1900	1600-1980	1901-1950	1951-1980	1981-2007
Alsace	Als	48.17	7.28	282.81	281.87	272.12	287.16	277.70
Bordeaux	Bor	45.18	-0.75	269.01	268.22	263.85	270.41	259.75
Burgundy	Bur	47.32	5.04	269.92	270.07	269.44	272.58	262.15
Champagne 1	Chal	47.98	4.28	266.88	267.52	267.01	270.02	264.92
Languedoc	Lan	43.60	3.87	272.43	270.28	260.97	266.88	263.40
Low Loire Valley	LLV	47.15	0.22	286.12	284.61	282.69	282.56	275.33
Southern Rhone Valley	SRv	43.98	5.05	269.20	269.10	268.84	268.46	257.87
Switzerland (Lake Geneva)	Swi	46.57	6.52	286.39	283.87	273.86	275.22	263.00

Table 2: For each regional grape harvest date series used in GHD-Core, the fraction of years with observations for various time intervals.

	1354-2007	1600-1900	1600-2007	1800-2007	1900-2007
Als	0.401	0.578	0.642	0.837	0.824
Bor	0.500	0.648	0.738	0.995	0.991
Bur	0.925	0.997	0.990	0.986	0.972
Cha1	0.280	0.259	0.449	0.880	0.981
Lan	0.442	0.635	0.689	0.438	0.833
LLV	0.310	0.332	0.498	0.976	0.963
SRv	0.690	0.970	0.951	0.942	0.898
Swi	0.749	1.00	1.00	1.00	1.00

Table 3: Spearman's rank correlations (1354-2007) between the various regional grape harvest date series used to construct GHD-Core.

	Als	Bor	Bur	Cha1	Lan	LLV	SRv	Swi
Als	1.00							
Bor	0.601	1.00						
Bur	0.574	0.615	1.00					
Cha1	0.632	0.675	0.799	1.00				
Lan	0.550	0.467	0.450	0.655	1.00			
LLV	0.503	0.712	0.776	0.709	0.359	1.00		
SRv	0.414	0.249	0.456	0.346	0.765	0.456	1.00	
Swi	0.604	0.554	0.562	0.569	0.705	0.697	0.501	1.00

Table 4: Day of year anomalies in the regional grape harvest date series used to construct GHD-Core. Anomalies are calculated relative to the baseline mean dates from 1600–1900. Also included are results for the GHD-Core index and GHD-All, composited from all 27 regional grape harvest date series in DAUX. For GHD-Core and GHD-All, the harvest date anomalies were calculated for the regional series individually before averaging together. Because the regional grape harvest date series are not all equally represented in all years, anomalies in GHD-Core and GHD-All are slightly non-zero for the baseline averaging period (1600–1900).

	1600-1900	1600-1980	1901-1950	1951-1980	1981-2007
Als	0	-0.94	-10.69	4.35	-5.11
Bor	0	-0.79	-5.16	1.40	-9.26
Bur	0	0.15	-0.48	2.66	-7.78
Chal	0	0.64	0.13	3.14	-1.96
Lan	0	-2.14	-11.46	-5.55	-9.03
LLV	0	-1.51	-3.42	-3.56	-10.79
SRv	0	-0.10	-0.36	-0.74	-11.33
Swi	0	-2.52	-12.53	-11.17	-23.39
GHD-Core	-0.32	-1.02	-5.16	-1.11	-10.24
GHD-All	-0.25	-0.85	-5.13	0.36	-8.91

Table 5: As Table 4, but for inter-annual standard deviation.

	1600-1900	1600-1980	1901-1950	1951-1980	1981-2007
Als	8.74	9.56	9.12	7.09	8.74
Bor	9.51	9.00	6.27	7.00	9.56
Bur	9.61	9.19	6.55	8.11	7.97
Chal	8.81	8.88	7.85	10.12	8.64
Lan	8.63	9.03	6.51	5.69	5.39
LLV	10.29	9.21	6.56	8.01	7.41
SRv	8.68	8.46	8.62	5.55	5.93
Swi	10.09	10.71	7.19	6.68	8.11
GHD-Core	7.67	7.49	5.39	6.24	7.10
GHD-All	7.03	7.02	5.55	6.55	6.75

Table 6: Coefficients and p-values from ordered logit models of wine quality data (on a scale of 0 to 5) and grape harvest dates (GHD) and CRU May-July seasonal temperatures for the periods 1900-1980 and 1981-2001. For more details on data and analyses see the Methods section in the main text.

	GHD: 1900-1980	GHD: 1981-2001	Temp: 1900-1980	Temp: 1981-2001
Red Bordeaux	-0.117 (<0.01)	-0.133 (0.03)	1.244 (<0.01)	1.308 (0.01)
White Bordeaux	-0.084 (<0.01)	-0.079 (0.14)	0.951 (<0.01)	1.109 (0.02)
Red Burgundy	-0.102 (<0.01)	-0.101 (0.18)	0.403 (0.06)	0.612 (0.23)
White Burgundy	-0.093 (0.02)	-0.144 (0.07)	0.564 (0.04)	1.262 (0.03)

Table 7: Coefficients and p-values from ordered logit models of wine quality data (on a scale of 0 to 5) and CRU May-July seasonal precipitation and Palmer Drought Severity Index (PDSI) for the periods 1900-1980 and 1981-2001. For more details on data and analyses see the Methods section in the main text.

	Prec: 1900-1980	Prec: 1981-2001	PDSI: 1900-1980	PDSI: 1981-2001
Red Bordeaux	-0.013 (<0.01)	-0.011 (0.12)	-0.457 (<0.01)	-0.119 (0.61)
White Bordeaux	-0.014 (<0.01)	-0.014 (0.06)	-0.291 (0.02)	-0.234 (0.32)
Red Burgundy	-0.018 (<0.01)	0 (0.96)	-0.273 (0.03)	0.12 (0.64)
White Burgundy	-0.011 (0.05)	-0.013 (0.08)	-0.101 (0.52)	-0.199 (0.41)

Table 8: Comparison of regression statistics between GHD-Core and the CRU climate data (May-June-July, MJJ) for 1901-1980. Shown are results for cases where all data was linearly detrended over time prior to the regression calculation (detrended) versus the case where no detrending occurred (normal).

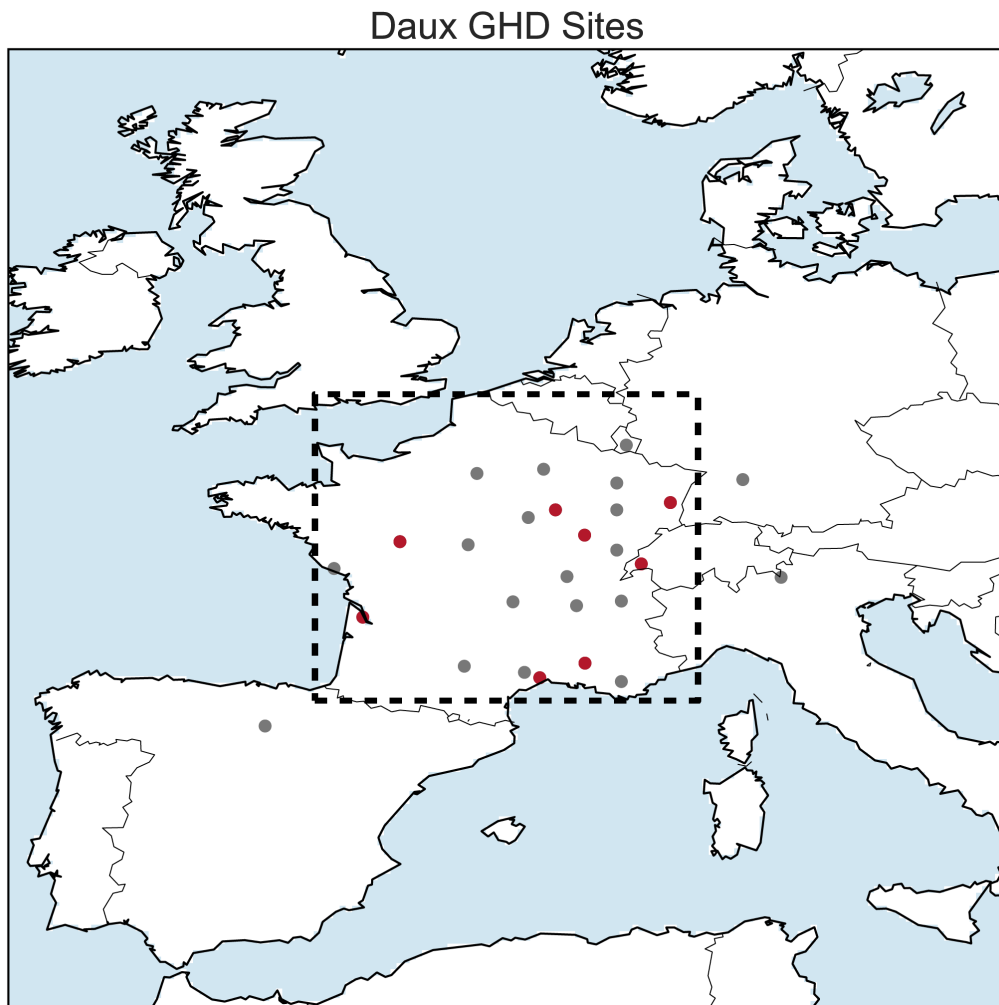
	Slope (normal)	Slope (detrended)	R2 (normal)	R2 (detrended)	p-val (normal)	p-val (detrended)
1901-1981						
Temperature	-6.044534	-6.218814	0.704	0.780	< 0.00000001	< 0.00000001
Precipitation	0.068827	0.068518	0.241	0.252	0.000004	0.000002
PDSI	1.682021	1.667401	0.133	0.137	0.000890	0.000709
1981-2007						
Temperature	-6.354566	-5.038086	0.642	0.473	0.000001	0.000073
Precipitation	0.033541	0.019836	0.051	0.030	0.258433	0.384498
PDSI	1.067015	0.429598	0.043	0.012	0.301859	0.592694

Table 9: Single and multivariate regressions between the CRU instrumental climate data (MJ, 1901–1980) and GHD-Core. Predictors are in the first column (temperature, precipitation, PDSI), followed by the coefficient of determination for the full regression model (R^2), Akaike Information Criteria (AIC), and regression coefficients and significance levels for the first (x1) and (where applicable) second (x2) and third (x3) predictors. The bottom two rows are for Temp+Precip and Temp+PDSI regression models with interactions terms

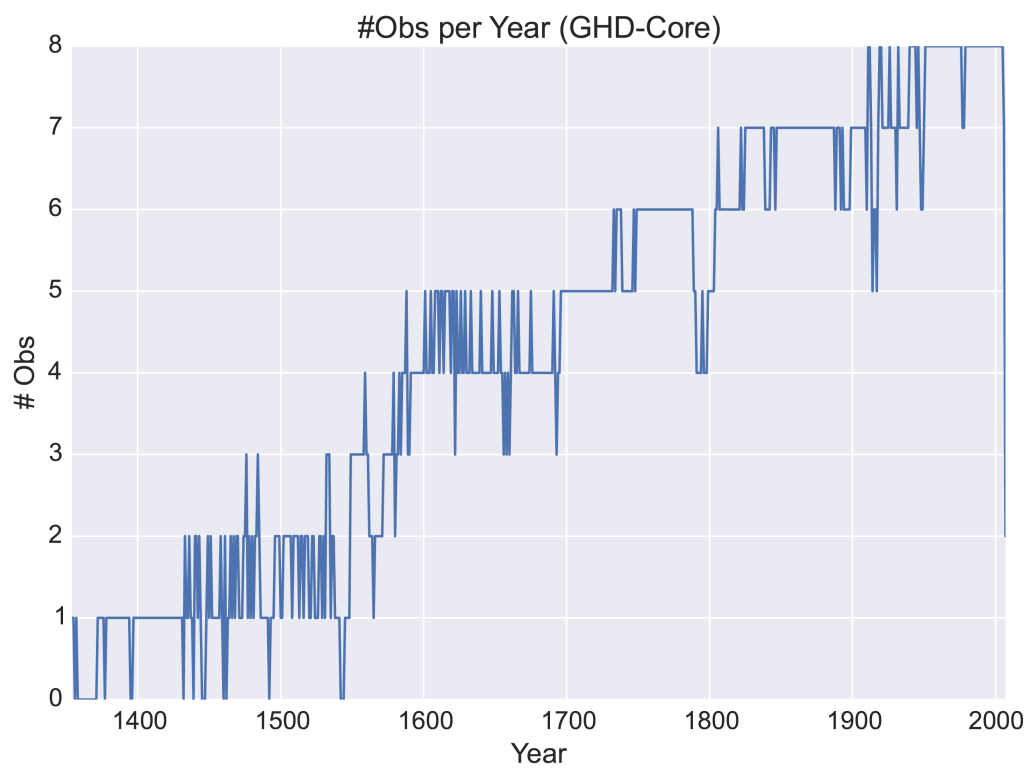
Predictor(s)	R^2	AIC	x1 (p)	x2 (p)	x3 (p)
Temp	0.704	421.72	-6.04 (< 0.001)	NA	NA
Prec	0.241	496.99	+0.07 (< 0.001)	NA	NA
PDSI	0.133	507.70	+1.68 (< 0.001)	NA	NA
Temp (x1) + Prec (x2)	0.713	421.27	-5.66 (< 0.001)	+0.02 (0.126)	NA
Temp (x1) + PDSI (x2)	0.706	423.08	-5.90 (< 0.001)	+0.24 (0.436)	NA
Temp (x1) + Prec (x2) + PDSI (x3)	0.713	423.26	-5.67 (< 0.001)	+0.02 (0.190)	-0.02 (0.946)
Temp (x1) + Prec (x2) + [Temp X Prec] (x3)	0.717	422.2	-3.90 (< 0.001)	+0.16 (0.270)	-0.01 (0.317)
Temp (x1) + PDSI (x2) + [Temp X PDSI] (x3)	0.708	424.53	-6.14 (< 0.001)	+4.06 (0.442)	-0.24 (0.468)

Table 10: As Table 9, but for the 1981–2007 period.

Predictor(s)	R ²	AIC	x1 (p)	x2 (p)	x3 (p)
Temp	0.642	158.68	-6.35 (< 0.001)	NA	NA
Prec	0.051	185.04	+0.03 (0.258)	NA	NA
PDSI	0.043	185.27	+1.07 (0.302)	NA	NA
Temp (x1) + Prec (x2)	0.677	157.94	-7.17 (< 0.001)	-0.03 (0.123)	NA
Temp (x1) + PDSI (x2)	0.647	160.3	-6.26 (< 0.001)	+0.37 (0.565)	NA
Temp (x1) + Prec (x2) + PDSI (x3)	0.728	155.27	-7.52 (< 0.001)	-0.06 (0.016)	+1.48 (0.048)
Temp (x1) + Prec (x2) + [Temp X Prec] (x3)	0.691	158.77	-11.96 (0.022)	-0.4 (0.286)	+0.02 (0.323)
Temp (x1) + PDSI (x2) + [Temp X PDSI] (x3)	0.658	161.52	-6.00 (< 0.001)	-10.34 (0.437)	+0.64 (0.420)

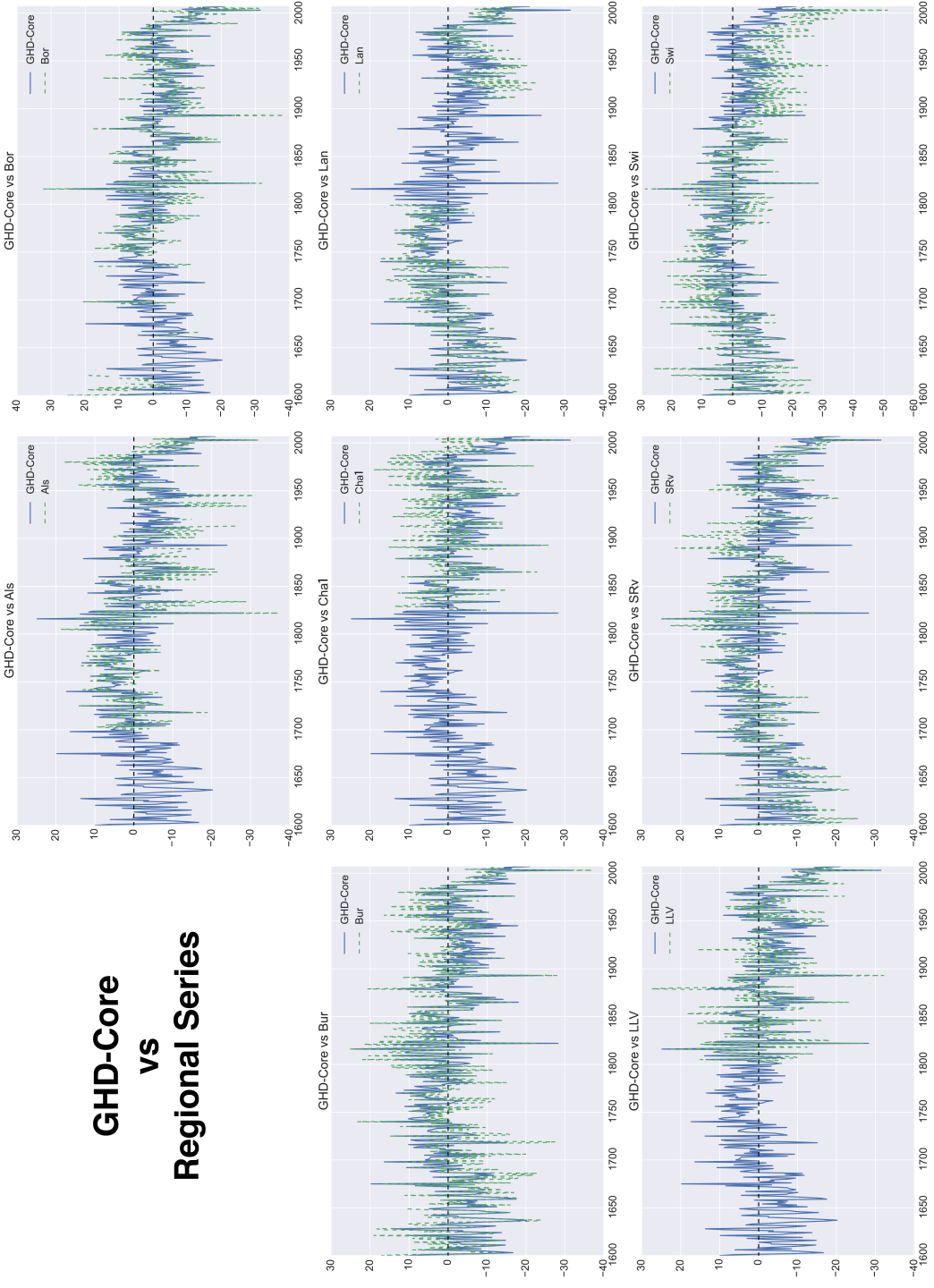


Supplementary Figure 1: Geographic locations for all 27 regional grape harvest date time series in DAUX. Highlighted in red are the sites that comprise the GHD-Core index: Alsace (Als), Bordeaux (Bor), Burgundy (Bur), Champagne 1 (Cha1), Languedoc (Lan), the Lower Loire Valley (LLV), the Southern Rhone Valley (SRv), and Switzerland at Lake Geneva (Swi). The dashed black box indicates the GHD-Core region (2°W – 8°E , 43°N – 51°N) over which climate anomalies from the CRU instrumental climate datasets and the three climate reconstructions were averaged for the various regression analyses.

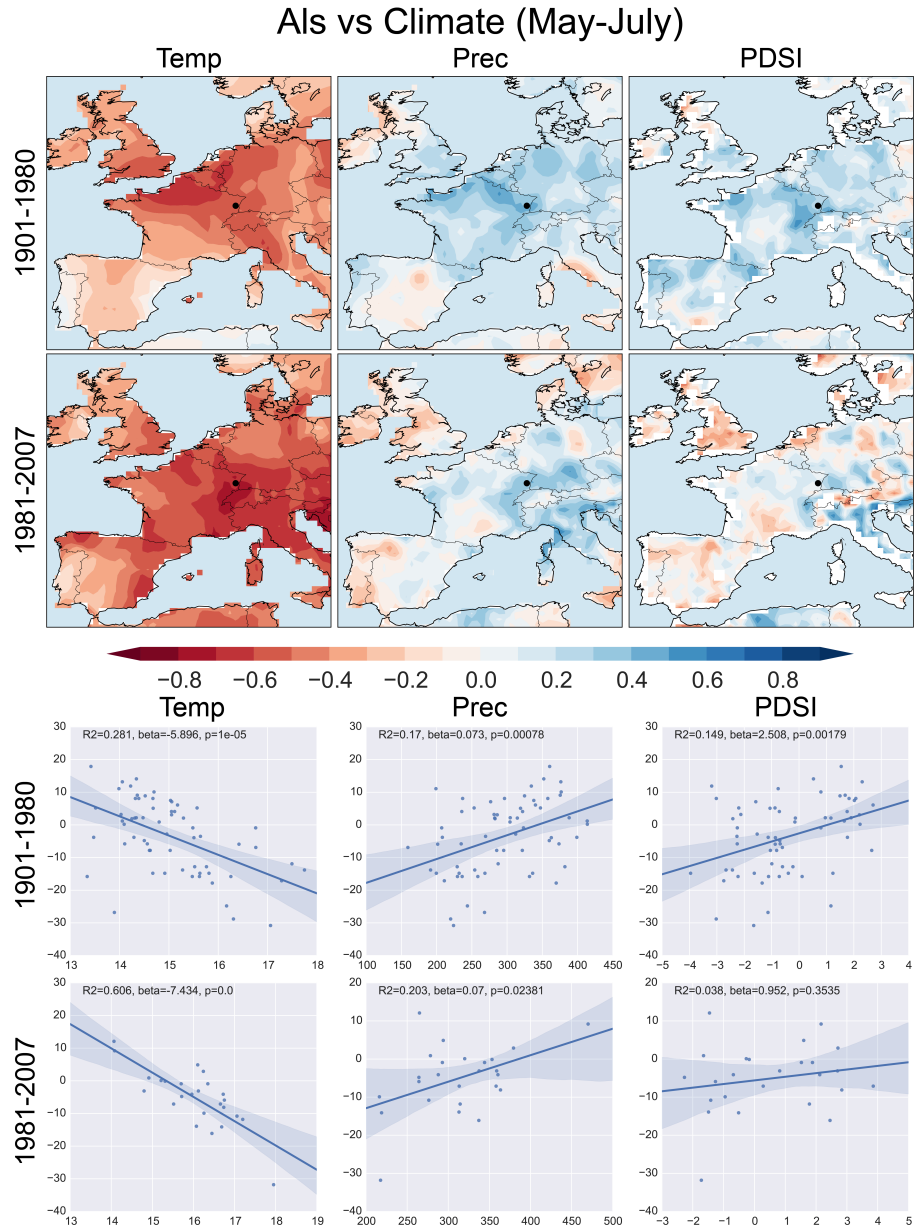


Supplementary Figure 2: Number of observations (i.e., regional grape harvest date series) represented in each year of the GHD-Core index.

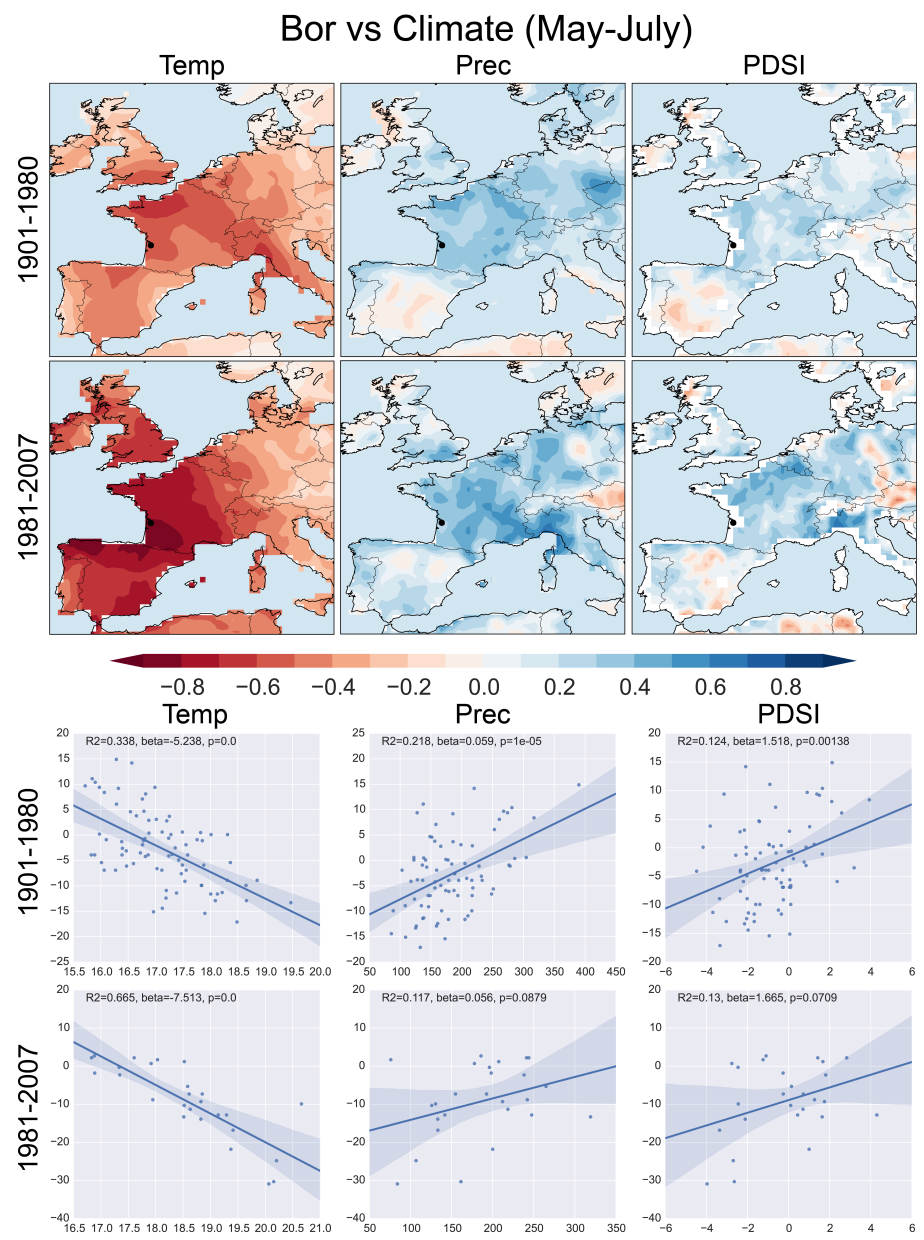
GHD-Core vs Regional Series



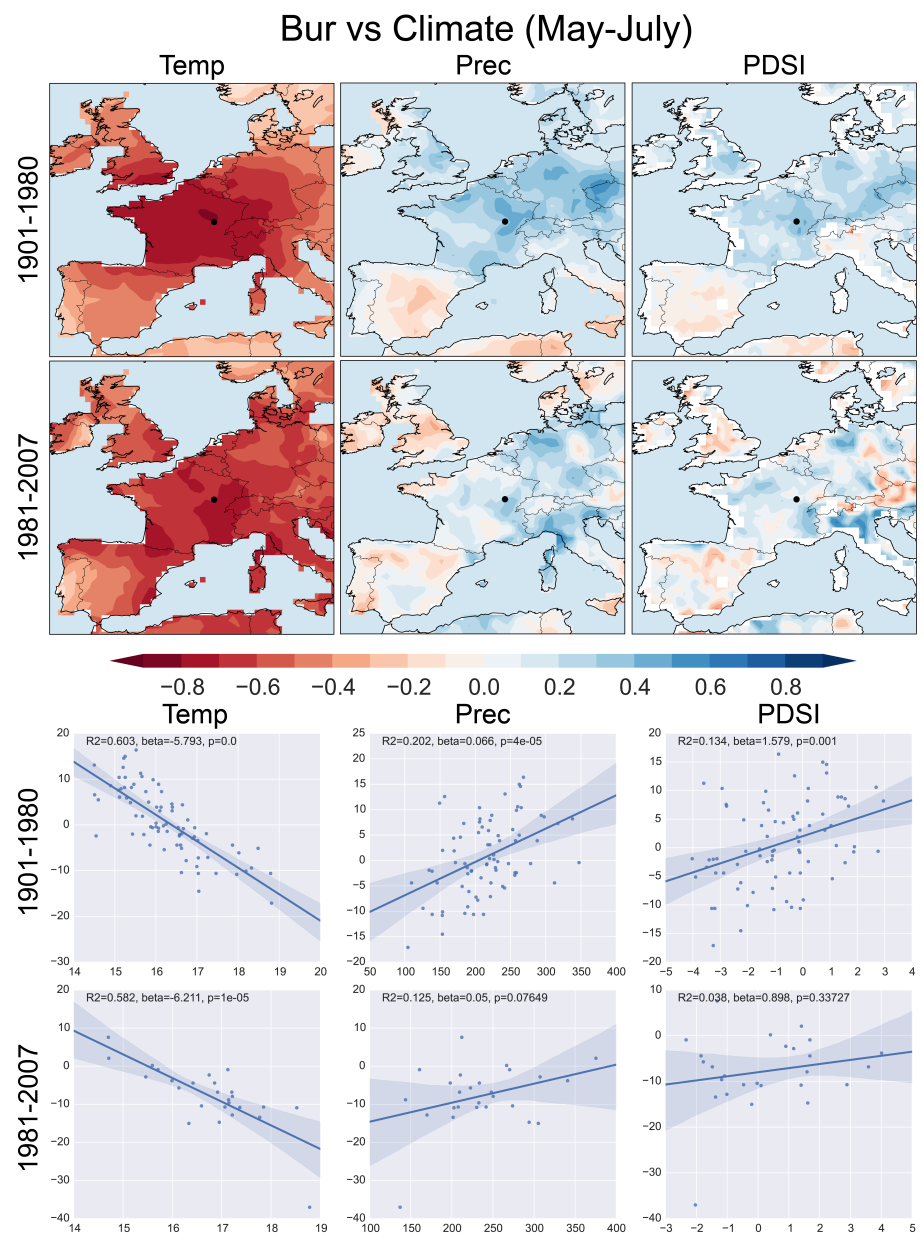
Supplementary Figure 3: Time series (1600–2007) of GHD-Core (blue solid line) and each individual regional grape harvest date series (green dashed lines) used in the construction of GHD-Core.



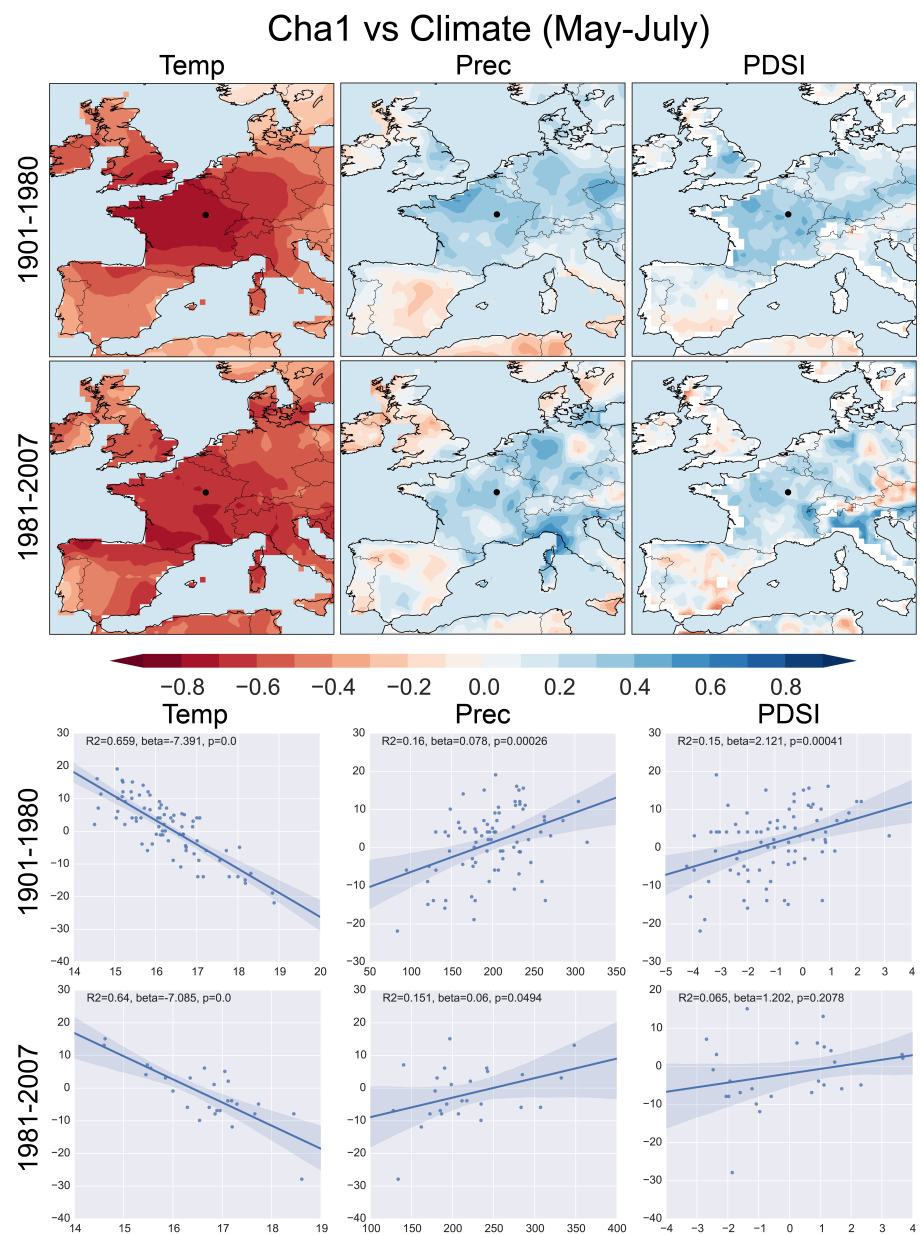
Supplementary Figure 4: Comparisons between the grape harvest date series from ALS and May-June-July temperature, precipitation, and PDSI from the CRU 3.21 climate grids. Top panels: point-by-point Spearman's rank correlations for 1901–1980 and 1981–2007 (location of ALS is shown by the black dot). Bottom panels: linear regression plots for the same intervals against CRU climate data averaged within one degree of the site location.



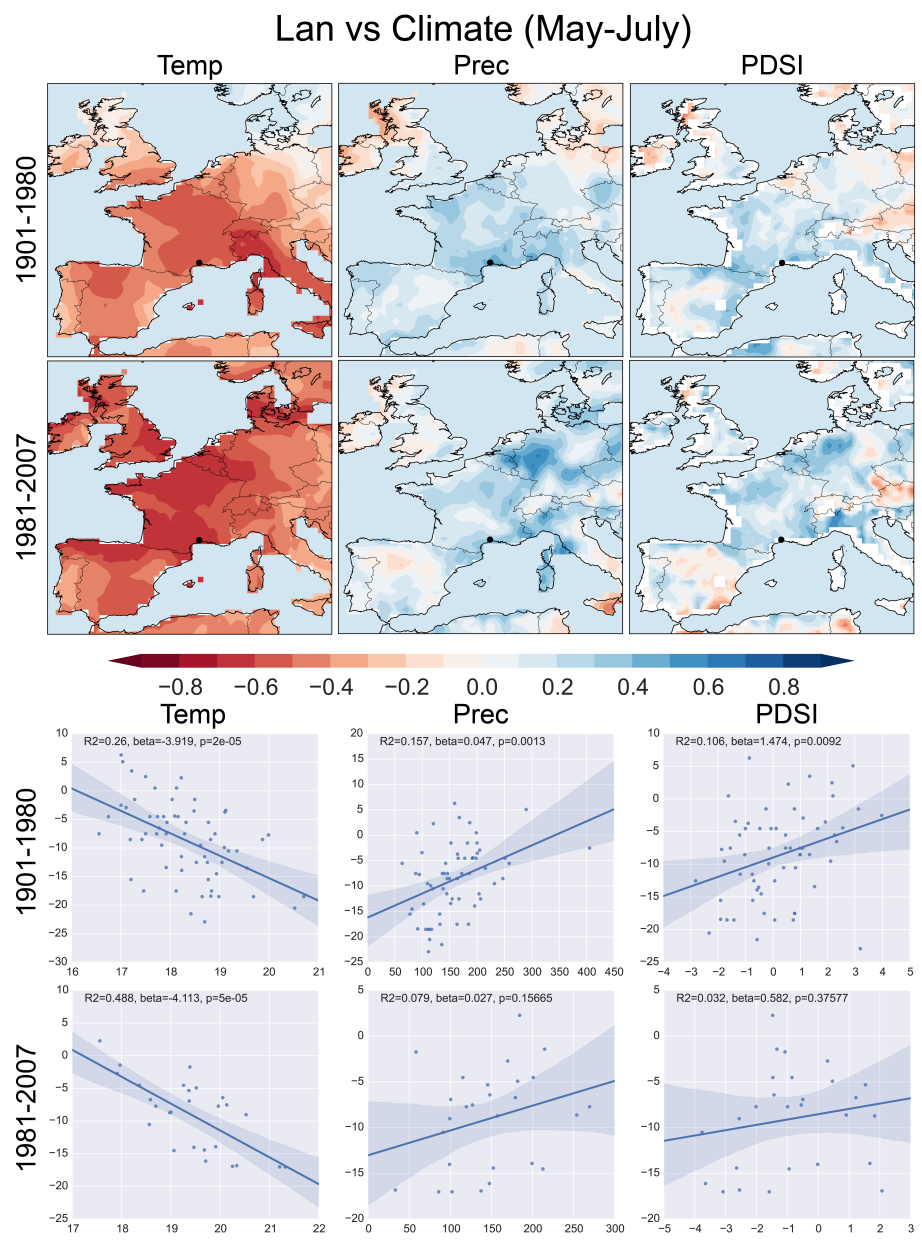
Supplementary Figure 5: Same as Figure 4, but for Bor.



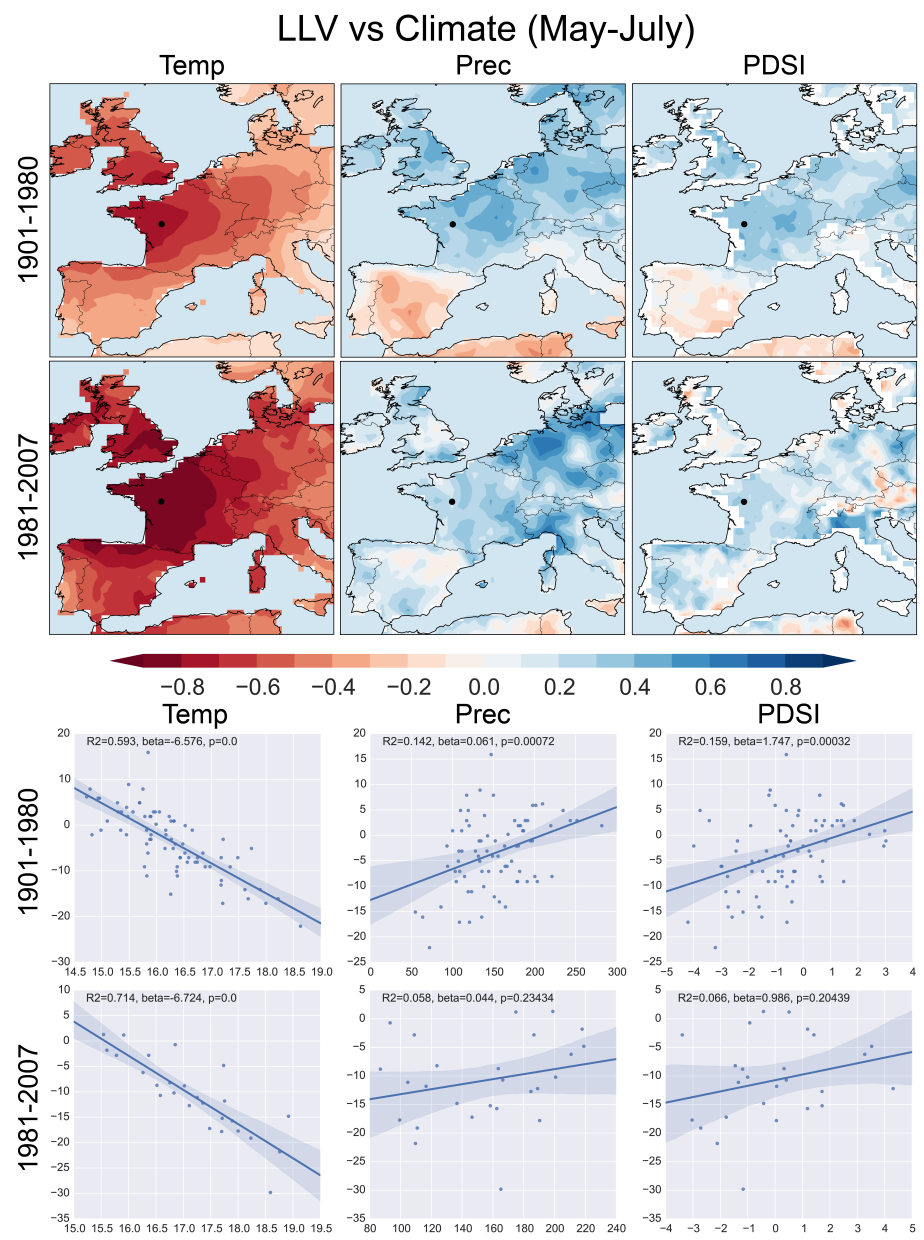
Supplementary Figure 6: Same as Figure 4, but for Bur.



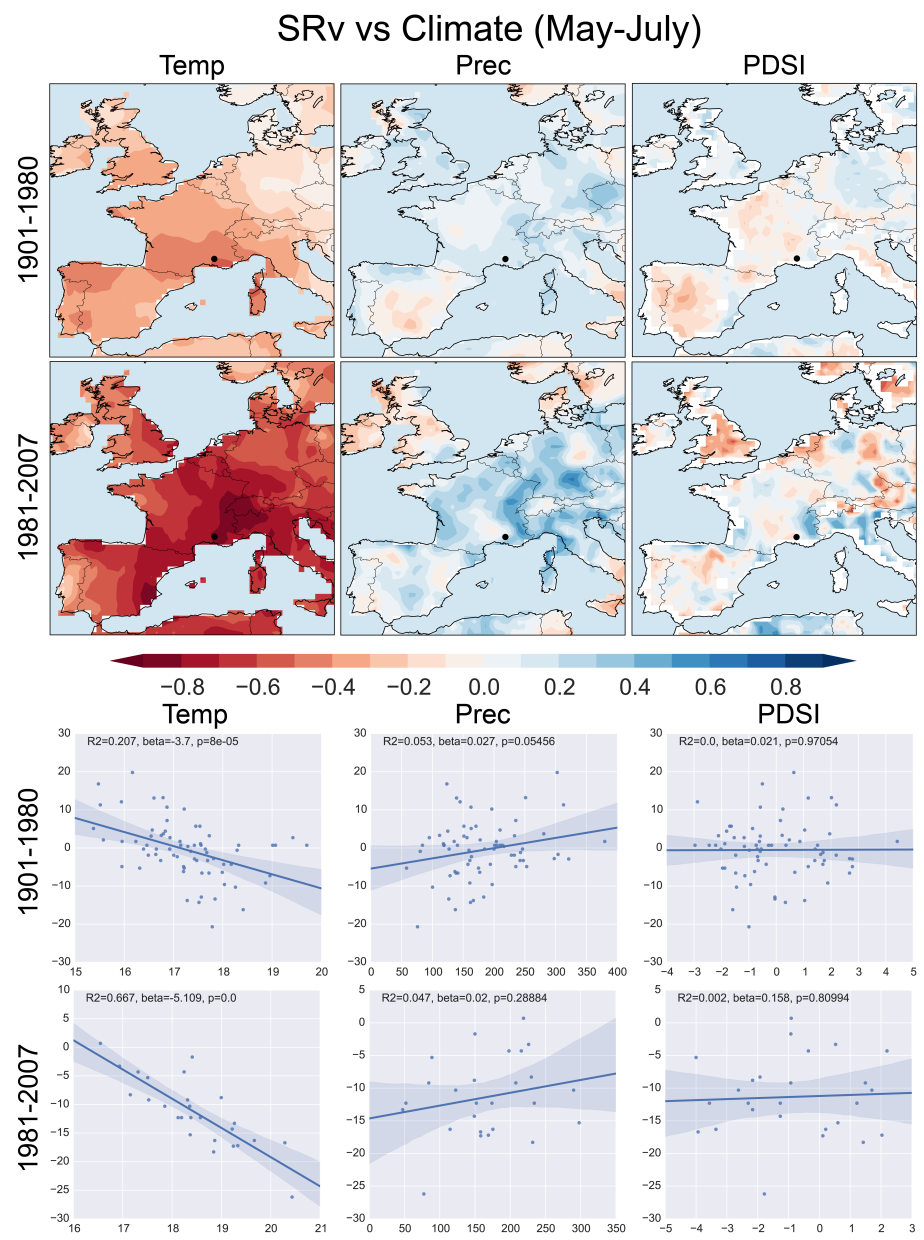
Supplementary Figure 7: Same as Figure 4, but for Cha1.



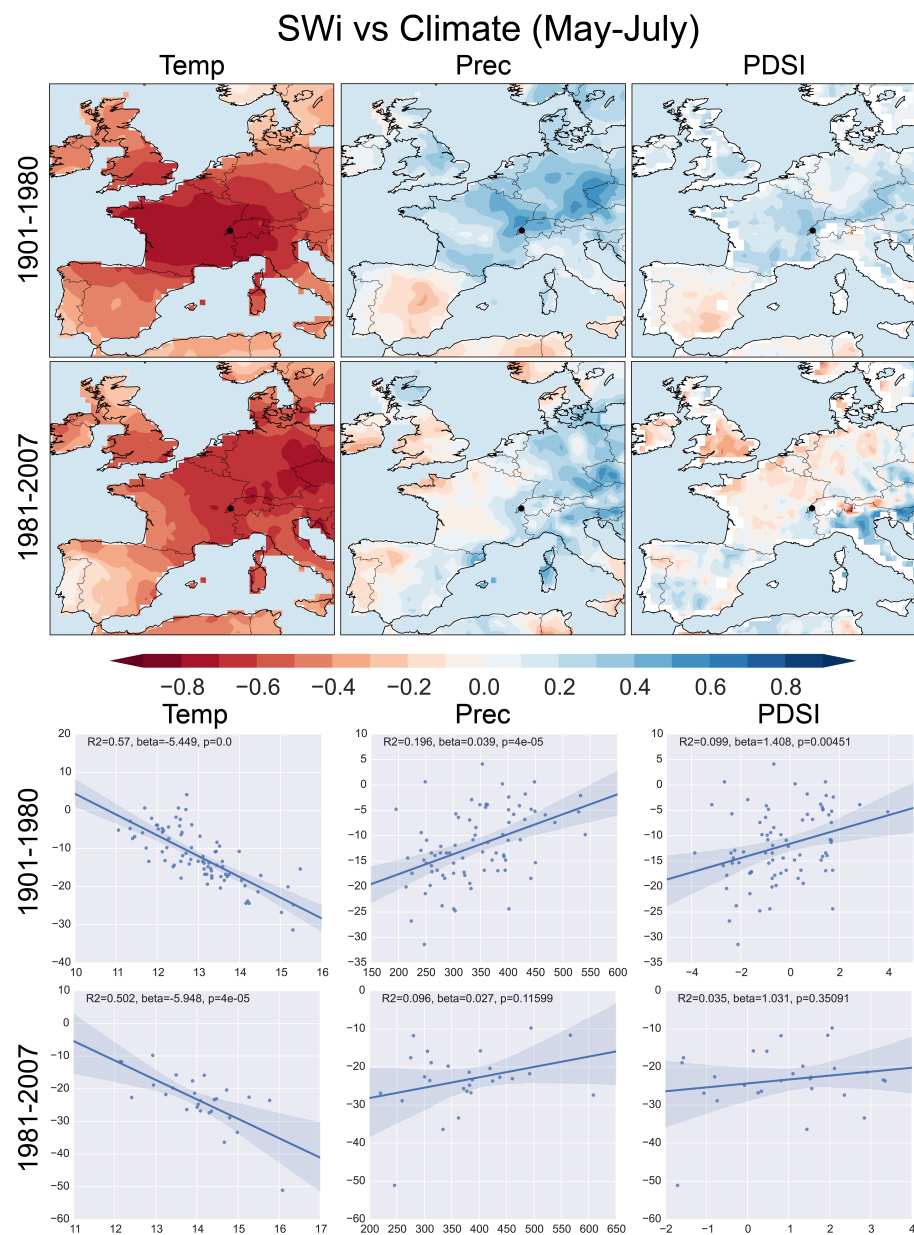
Supplementary Figure 8: Same as Figure 4, but for Lan.



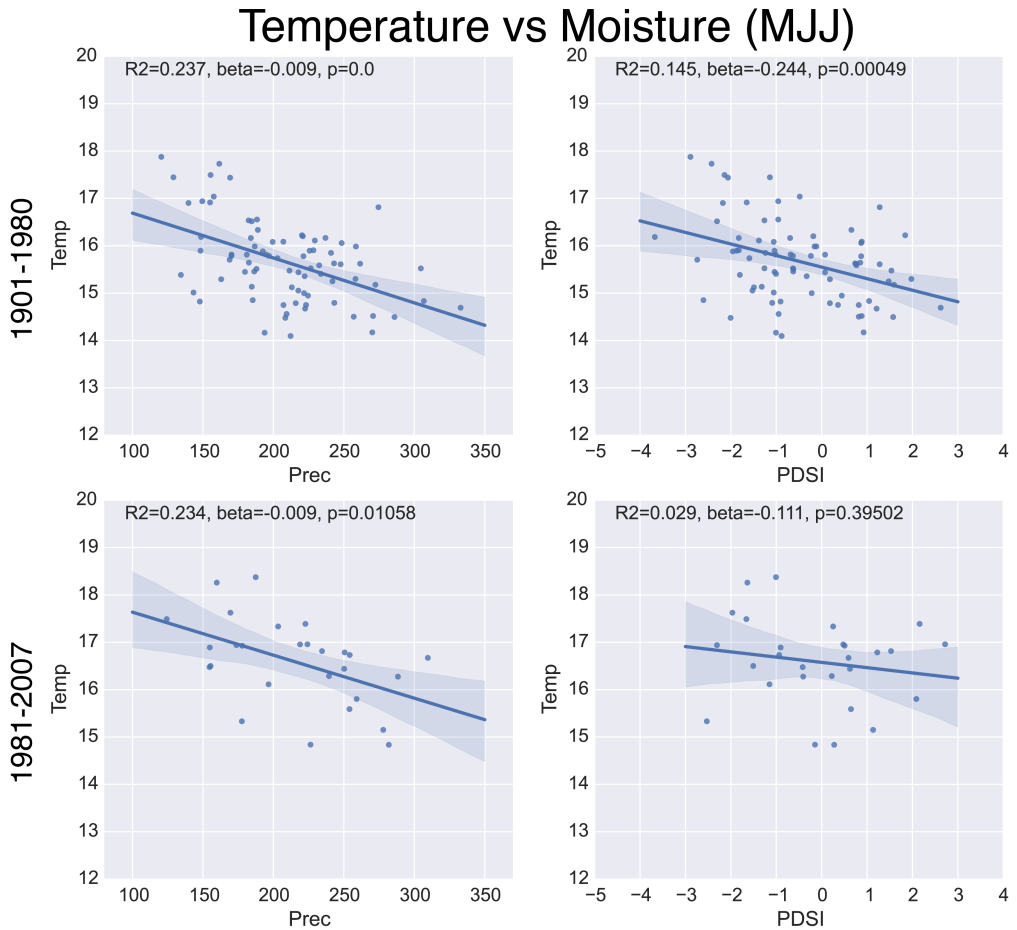
Supplementary Figure 9: Same as Figure 4, but for LLV.



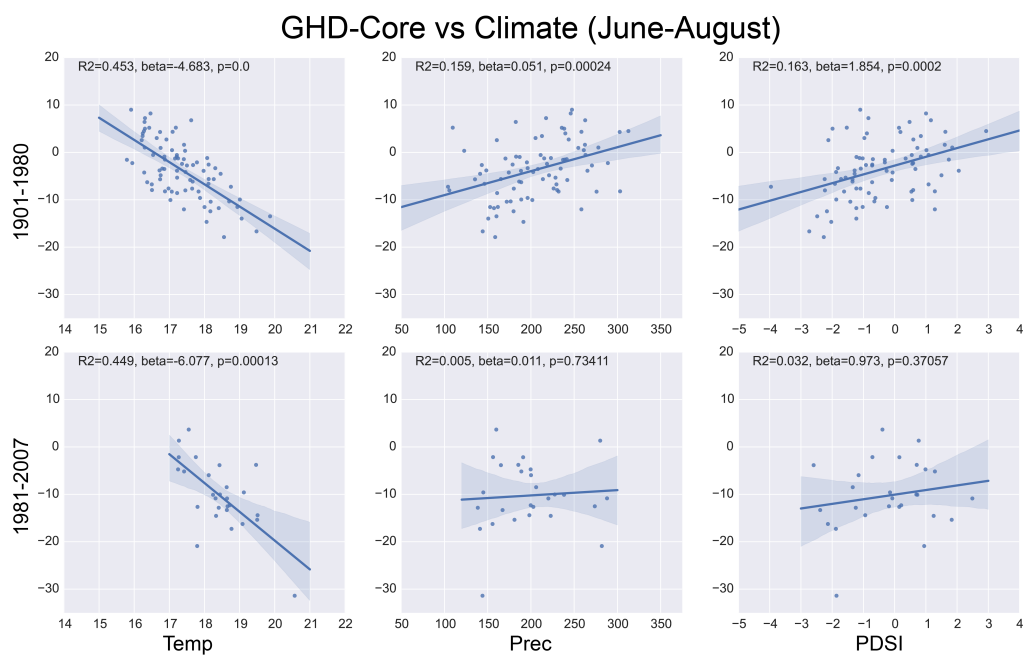
Supplementary Figure 10: Same as Figure 4, but for SRv.



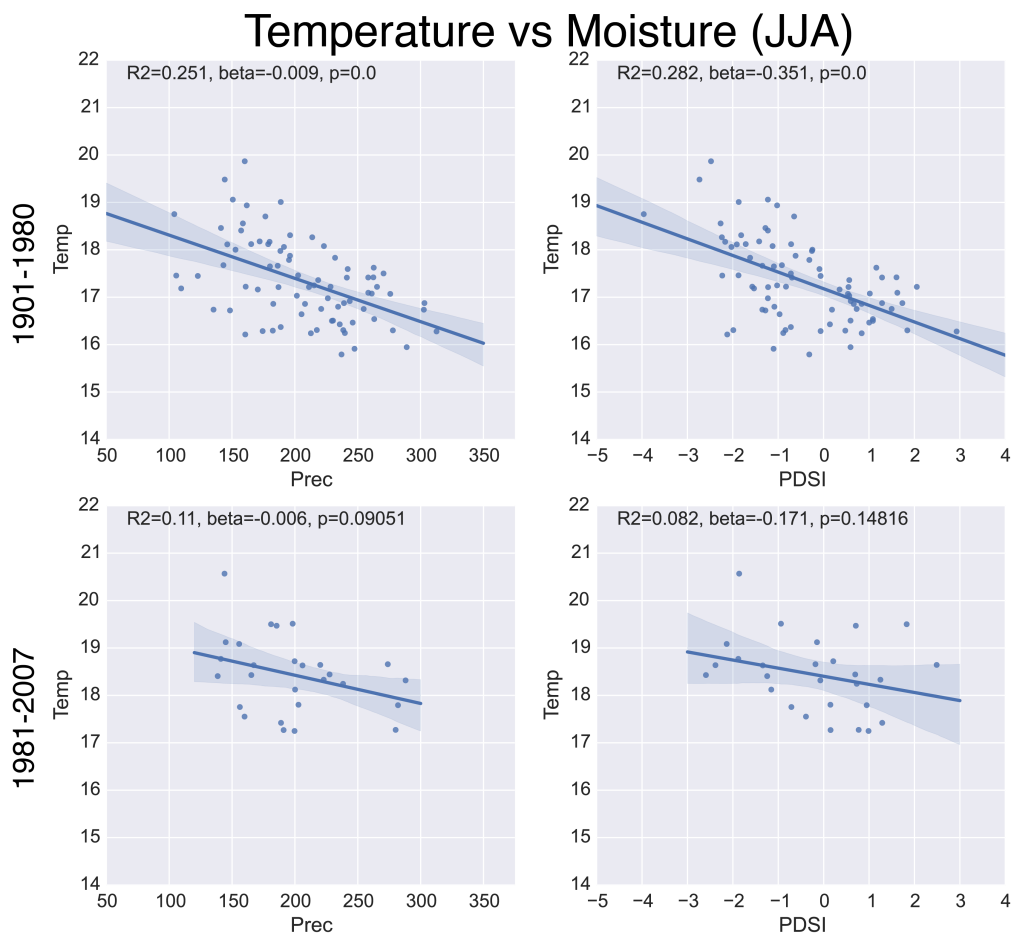
Supplementary Figure 11: Same as Figure 4, but for SWi.



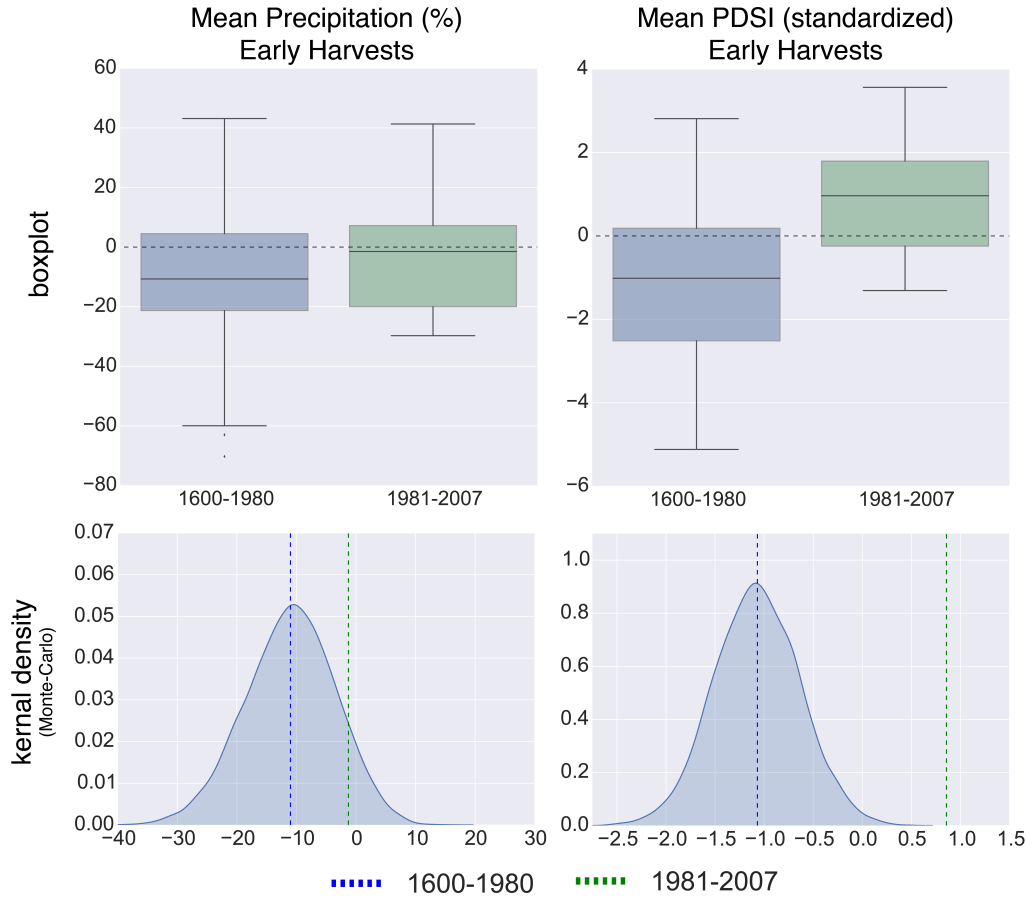
Supplementary Figure 12: Temperature versus moisture (precipitation and PDSI) during May-June-July for the GHD-Core region from the CRU 3.21 climate grids for two periods: 1901–1980 and 1981–2007. Temperature during MJJ has a significant negative relationship with both precipitation and PDSI, indicating the tendency for warmer conditions during drier years. Over the more recent period, the relationship between temperature and PDSI breaks down, but the relationship with precipitation remains largely consistent.



Supplementary Figure 13: Same as Figure 3 from the main manuscript, but for June-July-August (JJA) climate.

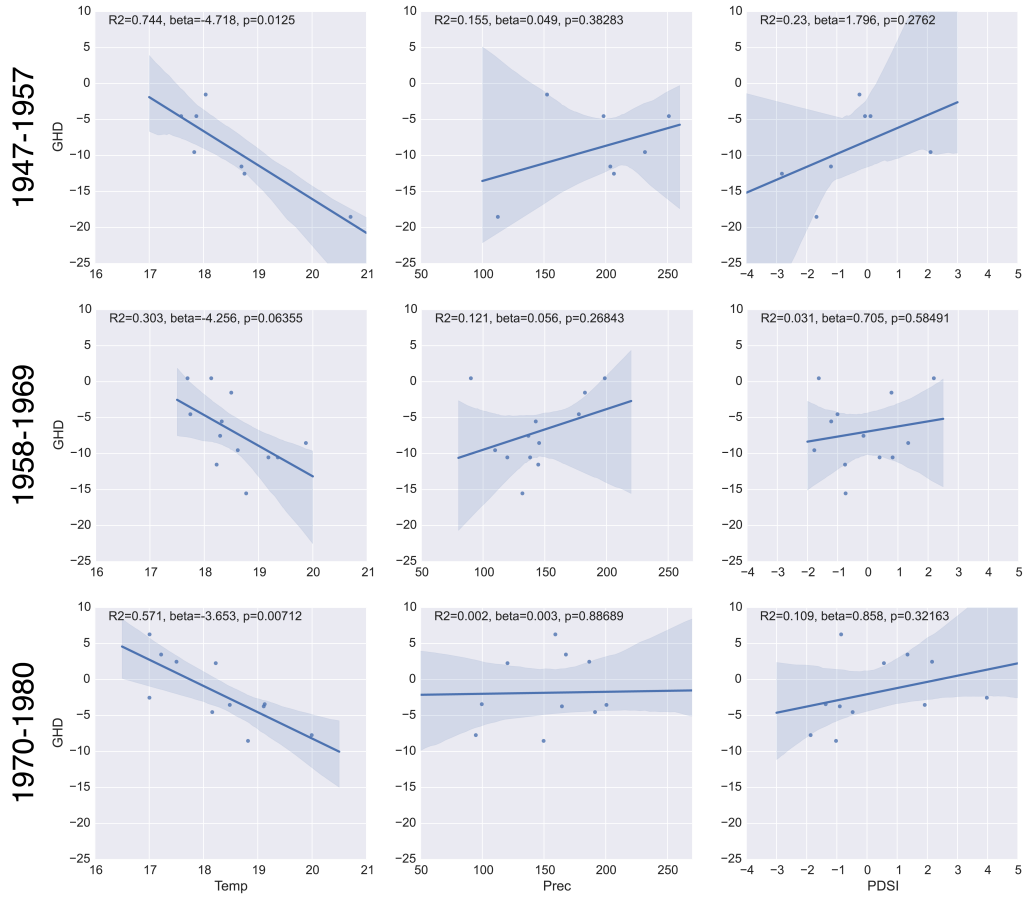


Supplementary Figure 14: Same as Supplemental Figure 12, but for June-July-August (JJA) climate. During JJA, the temperature moisture relationship is stronger over this region and, in both precipitation and PDSI, these relationships breakdown in the recent decades (1981–2007).

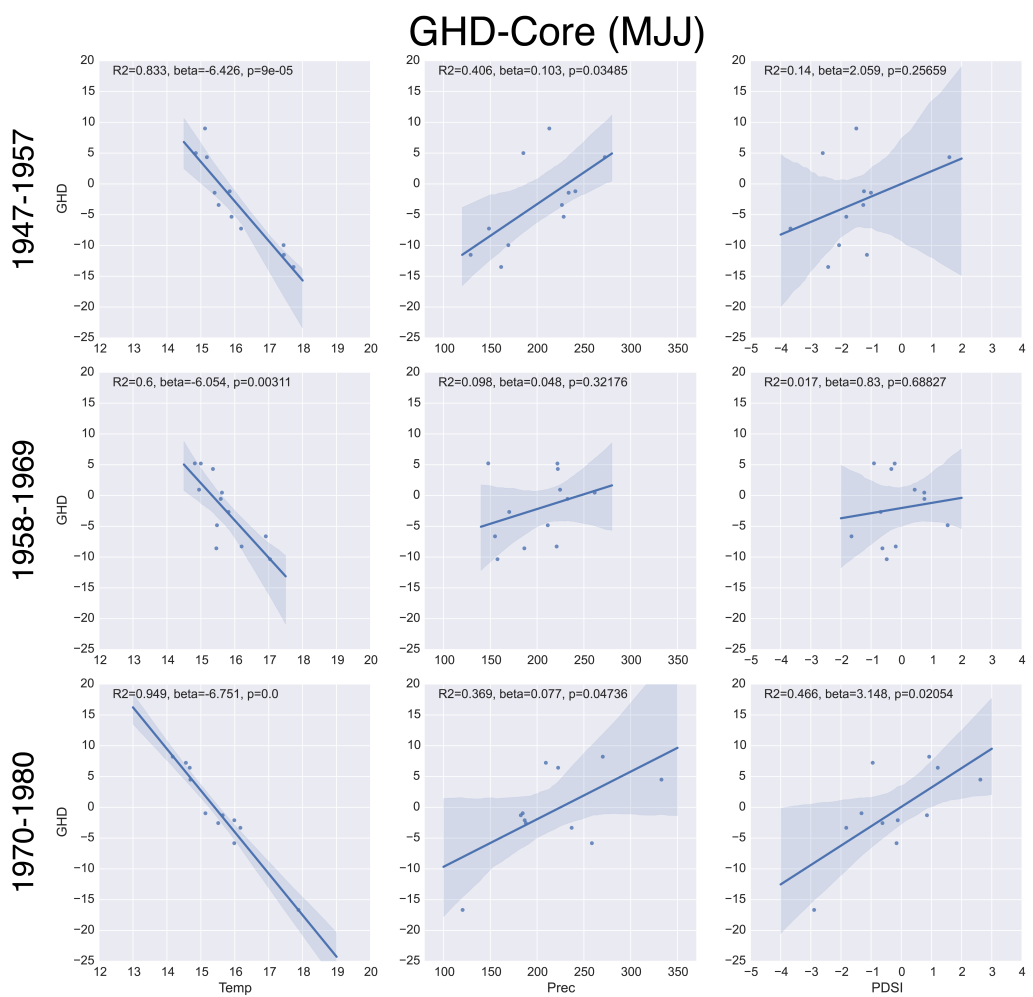


Supplementary Figure 15: Top row: box plots of pooled precipitation and PDSI anomalies from the climate reconstructions for years with early harvest date anomalies in GHD-Core. Bottom row: kernel density functions of recalculated mean precipitation and PDSI anomalies associated with early harvest dates, based on 10,000 Monte-Carlo resamplings with replacement. Dashed vertical lines represent the mean anomalies calculated from the actual early harvest years from 1600–1980 (blue) and 1981–2007 (green).

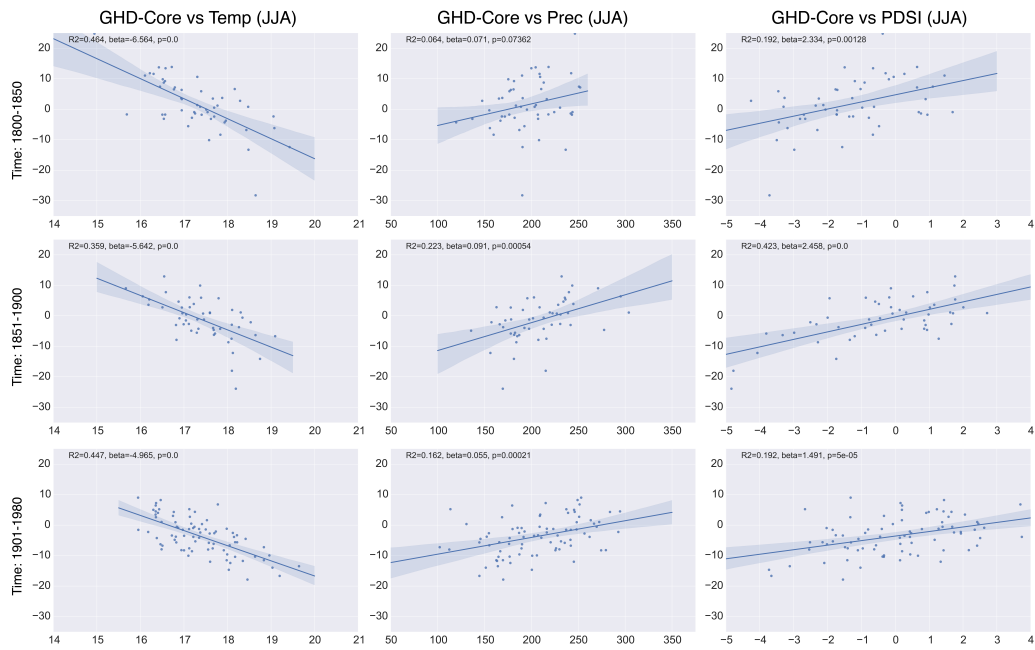
Languedoc (MJJ)



Supplementary Figure 16: Regressions between harvest date and the instrumental data (temperature, precipitation, PDSI) for the Languedoc regional series. Interval correspond roughly to a time period when significant clonal selection at Languedoc likely occurred.



Supplementary Figure 17: As Supplementary Figure 16, but for GHD-Core.



Supplementary Figure 18: Regressions between harvest date and the climate reconstructions data (temperature, precipitation, PDSI) for the GHD-Core composite series. Interval correspond to intervals prior to the introduction of phylloxera (1800–1850), during the infestation (1851–1900), and following the widespread grafting of French vines onto American root stock (1901–1980).